MARTIN MARIETTA ENERGY SYSTEMS LIBRARIES

3 4456 0350065 5

ornl

ORNL/TM-12081

OAK RIDGE
NATIONAL
LABORATORY

MARTIN MARIETTA

Thermal Energy Storage Technical Progress Report

April 1990–March 1991

J. J. Tomlinson

OAK RIDGE NATIONAL LABORATORY
CENTRAL RESEARCH LIBRARY
CIRCULATION SECTION
4500N ROOM 175
LIBRARY LOAN COPY
DO NOT TRANSFER TO ANOTHER PERSON
If you wish someone else to see this report, send in name with report and the library will arrange a loan.
ornl-rsh-rb 5-77

MANAGED BY
MARTIN MARIETTA ENERGY SYSTEMS, INC.
FOR THE UNITED STATES
DEPARTMENT OF ENERGY

ORNL/TM-12081
Dist. Category UC-202

ENGINEERING TECHNOLOGY DIVISION

THERMAL ENERGY STORAGE TECHNICAL PROGRESS REPORT APRIL 1990 - MARCH 1991

J. J. Tomlinson

Date Published - March 1992

Prepared for
Office of Renewable Energy
Al 10 01 00 0

Prepared by the
OAK RIDGE NATIONAL LABORATORY
Oak Ridge, Tennessee 37831
Managed by
MARTIN MARIETTA ENERGY SYSTEMS, INC.
for the
U.S. DEPARTMENT OF ENERGY
under contract DE-AC05-84OR21400

MARTIN MARIETTA ENERGY SYSTEMS LIBRARIES

3 4456 0350065 5

CONTENTS

Page

LIST OF FIGURES v
LIST OF TABLES vii
ABSTRACT 1
1. PROGRAM OVERVIEW 1
1.1 DIURNAL TES PROGRAM 3
1.2 INDUSTRIAL TES PROGRAM 5
2. TECHNICAL PROGRAM - DIURNAL TES 6
2.1 DEVELOPMENT OF COMPLEX-COMPOUND CHILL STORAGE SYSTEM 6
2.2 DIRECT CONTACT ICE SYSTEM DEVELOPMENT 8
2.2.1 System Description and Operation 9
2.2.2 Instrumentation 10
2.2.3 Test Procedure 10
2.2.4 System Performance 12
2.2.4.1 Charging Performance 12
2.2.4.2 Discharging Performance 13
2.2.4.3 Equipment Performance 15
2.3 PCM WALLBOARD DEVELOPMENT 16
2.3.1 PCM Wallboard Fire Safety Studies 17
2.3.1.1 Reduced Levels of PCM 17
2.3.1.2 PCM Wallboard Covered with a Nonflammable Surface 17
2.3.1.3 Flame Suppression Using Fire Retardants 18
2.3.2 Alternatives to PCM Imbibing Process 20
2.3.3 PCM Wallboard Computer Simulation and Validation 22
2.4 EFFECTS OF DOPANTS ON SOLID-STATE PCMS 28
3. TECHNICAL PROGRAM - INDUSTRIAL TES 32
3.1 DEVELOPMENT/TESTING OF TES MEDIA FOR INDUSTRIAL APPLICATIONS 32
4. CONCLUSIONS 34
REFERENCES 36

LIST OF FIGURES

Figure		Page
1	Ammonia adsorption rate in 4 ton-h reactor.	8
2	Schematic of direct contact ice maker.	9
3	Direct contact ice making performance	14
4	Tank leaving water temperatures during melting.	15
5	Steiner tunnel test results of PCM wallboard.	19
6	PCM wallboard testing in the UTHA	23
7	Comparison of WALL88 with experimental transient	24
8	Comparison of WALL88 to known analytical solution.	25
9	Comparison of WALL88 to experimental transient data; Assumed melting point: 74° F.	26
10	DSC plot for the paraffin blend used in this project.	27
11	Heat capacity relation used to simulate a melting range.	28
12	Comparison of modified WALL88 to experimental transient data.	29
13	Phase diagram for PE/NPG system.	30
14	Phase diagram for the AMPL/NPG system.	31
15	Schematic of packed bed test facility.	33

LIST OF TABLES

Table		Page
1	Summary of direct contact ice making tests	13
2	Summary of ice melting tests	16
3	Water pick-up of plaster cubes (USG) with hydrophilic silica/PCM and hydrophobic silica/PCM	21

THERMAL ENERGY STORAGE TECHNICAL PROGRESS REPORT
APRIL 1990 - MARCH 1991

J. J. Tomlinson

ABSTRACT

The Department of Energy (DOE) is supporting development of thermal energy storage (TES) as a means of efficiently coupling energy supplies to variable heating or cooling demands. Uses of TES include electrical demand-side management in buildings and industry, extending the utilization of renewable energy resources such as solar, and recovery of waste heat from periodic industrial processes. Technical progress to develop TES for specific diurnal and industrial applications under Oak Ridge National Laboratory's TES program from April 1990 to March 1991 is reported and covers research in the areas of low temperature sorption, direct contact ice making, latent heat storage plasterboard and latent/sensible heat regenerator technology development.

---

1. PROGRAM OVERVIEW

Thermal energy storage consists of a range of technologies that allow an energy supply to be coupled to a heating or cooling demand. Acting as a buffer, TES facilitates the use of a time-varying energy resource to meet a constant or variable demand for heat or cool. Alternatively, TES is used to store available energy as sensible or latent heat in a material to meet an energy demand occurring at a later time. There are several advantages afforded by the use of TES including: (1) reduced sizes for heating and cooling systems in buildings, (2) load management of electricity used for heating and cooling, (3) waste heat utilization, and (4) renewable energy use.

In the case of buildings, heating and cooling systems are sized to maintain occupant comfort on design days during summer and winter. Design days are defined such that the probability of experiencing actual weather and load conditions worse than design day conditions is very small. Therefore, typical heating and cooling systems are oversized and consequently underutilized for most of the time so that they operate either cyclically or at reduced capacity. A TES system coupled to downsized heating/cooling plants allow them to be operated continuously so that they can meet a thermal demand that is much larger than the installed capacity. The overall result is a smaller and less costly heating/cooling system that operates most of the time at its most efficient rating. This feature can also be used when a building is expanded; TES increases the duty cycle of the existing space conditioning system so that the larger peak thermal load can be met with no increase in installed capacity.

A second benefit of TES in buildings is that it provides flexibility in scheduling heating and cooling system operation. That is, the TES system can respond to the space conditioning demands of the building, and the heating/cooling system can be operated independently or on a fixed schedule. In the case of electric chillers, heat pumps or resistance heating systems, this TES feature can be an advantage to a customer interested in avoiding on-peak electric costs as well as to the electrical utility interested in shifting load from certain times of the day. Due to rapid electric load growth caused by commercial building air conditioning, utilities are providing an opportunity for cool TES in the form of cash incentives, TES feasibility studies and rate schedules that encourage implementation of thermal storage.

Industrial applications for TES include processes in which waste heat generation is noncoincident with a heating demand. By storing heat that is otherwise wasted in flue gas, a TES system permits this energy to be reused in processes such as drying or preheating. The result is an overall reduction in energy requirements of industry and a reduction in thermal emissions from individual plants.

Solar energy used for space heating or cooling usually requires a TES system to extend the solar resource to nighttime periods. Conventional solar TES systems consisting of masonry or stored water are based on sensible heat in which the energy stored is directly proportional to the change in temperature of the storage material. These materials located on the interior of a building can overheat the occupied space unless relatively large TES masses are used. Depending on climate and the cost of fuel, these systems can be uneconomic and are particularly unsuited for retrofit applications. Advanced TES systems use the latent heat of solid-liquid or solid-solid transformations in phase change materials (PCMs). These transformations are energetic and occur over a relatively small temperature range—an advantage for a TES system that is charged or discharged by room air.

The DOE TES program has continued research to develop and support commercialization of TES technologies for each of these application areas. The cycling frequency for TES systems aimed at solar applications, and demand reduction during electrical off-peak periods is diurnal, whereas the cycling frequency for industrial applications of TES is less restrictive. For these reasons, TES research is arranged into the two broad areas: diurnal TES and industrial TES.

1.1 DIURNAL TES PROGRAM

The diurnal TES program is aimed at the development of TES materials and systems for specific applications. A principal project within the diurnal program is the development of a chill storage system that can be used to provide off-peak refrigeration in the -40°C (°F) to -7°C (20°F) range. All refrigerated warehouses, food processing and many chemical processing plants require refrigeration in this temperature range, most of which is electrically driven. A chill TES system permits the compressor load to be removed from the on-peak period and cooling is provided either continuously or on a schedule and at a rate that is controlled by the process or storage conditions. Under contract to Martin Marietta Energy Systems, Inc., the Rocky Research Company is working to develop a chill TES system based on sorption of ammonia by a salt to produce an ammoniated complex compound.[1] During the charging process, a compressor draws ammonia from a complex compound inside a reactor; the ammonia is condensed and stored in a refrigerant receiver. At the end of the charging process, most of the ammonia in the system resides in the receiver leaving the salt in the reactor with a low ammonia concentration. During the discharging process, the ammonia in the receiver evaporates with heat from the cooling load and returns to recombine with the salt in the reactor. Ammonia movement in the discharge process occurs without compressor operation due to the pressure difference between the receiver and reactor. During the charging process, the compressor drives ammonia vapor from the reactor to the condenser/receiver subsystem. The fact that the chill TES system uses ammonia is a key advantage since ammonia is a refrigerant of choice in many industrial cooling systems. Details of recent technical results in this project are described in Section 2.1.

A second major program initiative is the development of an advanced TES system for building cooling with off-peak electricity. As mentioned earlier, there is growing interest in cool storage for buildings, and ice storage systems are being installed and used to provide off-peak cooling. In these systems, ice is frozen to an evaporator surface and must either be removed and stored in a tank to be useful, or is slowly melted away from the heat exchange surface during discharge to deliver cooling where needed. In the case of dynamic ice making, the ice formed on a cooled plate and when the thickness of ice reaches approximately 0.6 cm (1/4 in.), the plate is defrosted and the ice drops into a bin for storage. This requires a

defrost mechanism and extra energy for defrosting. In other systems where the ice remains frozen to a surface and undergoes external or internal melt for discharge, large, extended surface heat exchangers are required to keep approach temperatures relatively small. Direct contact between an evaporating refrigerant and water is one method for increasing the heat transfer rate and eliminating the need for a heat transfer surface. Research is underway at CBI Technical Services Company (CBI) to develop a direct contact ice storage system and to measure its performance. The system is operated by sparging evaporating refrigerant against a stream of water. Ice crystals fall into a tank, and the refrigerant vapor returns to the compressor. The water carryover issue is being accommodated by CBI using a new compressor technology unique to the cooling application. During the reporting period, a prototype direct contact ice storage system was designed, built and tested in the laboratory. A detailed description of this unique system, the performance of this system as determined in CBI's laboratory, and an assessment of prospects for ultimate commercialization of the direct contact system are given in Section 2.2.

A third major initiative is the development of building materials with enhanced heat capacity. Although early techniques for using containerized PCMs in buildings have been examined, commercialization of these concepts have foundered due to the added expense of engineering them into standard structures, or in the case of latent heat storage in some PCMs, stability problems. A promising approach to resolve both of these issues is the incorporation of congruently melting PCMs into conventional building materials. Using the building material itself to hold the PCM eliminates the need for a separate container, and using congruently melting PCMs improves the effective lifetime of the concept. An approach being examined by the University of Dayton Research Institute (UDRI) uses a paraffin PCM contained in the matrix of standard gypsum plasterboard. Prior work has shown[2] that once the PCM is inside the plasterboard, it is effectively contained (even when melted) by surface forces between the PCM and the large area provided by the needles of gypsum in the core of the plasterboard. This work also identified a paraffin blend that melts and freezes at approximately 22°C (72°F), which is in the room temperature range, and also identified and tested an immersion method for incorporating the PCM into the plasterboard. Plasterboard manufacturers have not shown as much interest in the immersion process for the PCM wallboard as a method whereby the PCM could be added to the wet plasterboard mix during manufacture. Therefore, efforts were focused on examining methods for preparing the PCM

as a dry powder that could be added as proposed. This work showed that the paraffin PCM could be added to certain finely divided silica to produce a dry powder even at temperatures above the melting point of the PCM. The dry powder is about 70 - 80 wt. % PCM. Other work during the reporting period focused on tests to identify the fire safety and flame spread characteristics of the PCM wallboard. While some tests were qualitative and conducted in the laboratory on small samples, a Steiner tunnel made available to the project by National Gypsum Company was used to perform fire testing according to ASTM E-84 procedures. The results of these tests showed the expected result that flammability increases with PCM concentration, and at a PCM concentration of 15 wt. %, the PCM wallboard has flammability characteristics similar to hardwood. These studies are continuing.

Experiments were conducted to determine the transient thermal response of PCM wallboard using a flat bed heating assembly at ORNL, and to correlate the measured thermal response with an analytical model of the PCM wallboard. Agreement between model and experiment during PCM melting was obtained when PCM thermophysical property data were taken from a differential scanning calorimeter (DSC) melting curve of the PCM rather than from theoretical melting behavior and from a "textbook" value for the melting point of the PCM. Further details of these findings is given in Section 2.3.

In addition to latent heat storage through freezing and melting of a PCM, latent heat can be stored and released through crystallographic changes in a solid material. As companion research to the PCM wallboard study using paraffin, the University of Nevada - Reno is engaged in a research project to understand and describe solid-solid transitions that occur in certain polyalcohol systems. Based on this understanding, dopants were identified and added to a material with a high solid-solid transition temperature to lower this transition to the room temperature range without a disproportionate loss in the heat of transition. The phase behavior of two binary alloys of selected polyalcohols was developed and is reported in Section 2.4.

1.2 INDUSTRIAL TES

Industrial TES consists of technologies used to capture available waste heat for reuse in an industrial process. For several years, the industrial TES program has continued

development of a composite TES material that, as pellets, could be used in a packed bed regenerator. The material, a composite consisting of a ceramic matrix suffused with a eutectic, was carried through laboratory development by the Institute of Gas Technology in prior years.[3] Later analytical studies on the predicted performance of a packed bed of composite material were conducted by Mississippi State University (MSU). During the reporting period, MSU completed the design of a high temperature packed bed TES test facility suited for testing the composite material under actual flue gas conditions. The completed design was submitted to a vendor for fabrication and shipment to the MSU campus. This work and a schematic of the test facility are given in Section 3.1.

2. TECHNICAL PROGRAM - DIURNAL THERMAL ENERGY STORAGE

2.1 DEVELOPMENT OF COMPLEX-COMPOUND CHILL STORAGE SYSTEM

The objective of this project is the development of a low temperature TES system for off-peak refrigeration applications. These applications are found mainly in food processing and storage industries where temperature levels of -7°C (19°F), -28°C (-18°F) and -40°C (°F) are used. The TES system under study uses the chemisorption of ammonia in a tank of solid salt. The presence of the salt reduces the equilibrium vapor pressure in the ullage and the ammonia vapor is taken up by the salt in an exothermic reaction. This heat of adsorption is removed by heat exchangers located in the salt. These heat exchangers are also used to provide heat to the ammoniated salt—or complex compound, driving the ammonia vapor from the salt in an endothermic reaction. The ammonia is then condensed and stored in a receiver vessel. Previous phases of this project conducted by the Rocky Research Company demonstrated in the laboratory the capability for adsorption and desorption of ammonia with average approach temperatures of around 5°C (9°F). The size of the laboratory system was 12.6 kJ (1 ton-h) of chill storage at -28°C (-18°F). The objectives of the current phase of the project were to demonstrate technical viability of increasing the scale of experiments to a single reactor with a TES capacity over 50 kJ (4 ton-h) and to demonstrate the feasibility of factory assembly of a complex compound reactor.

The current phase of the project was accomplished as a joint effort between Rocky Research Company and Standard Refrigeration Company (Chicago). A single reactor was

designed, constructed and coded as a pressure vessel by Standard using industry practices for tube-in-shell heat exchangers. The cylindrical vessel was 0.6 m (2 ft) in diameter and 1.52 m (5 ft) long. The internal heat exchanger modules were supported by tube sheets at each end of the vessel, and baffles in the heads were used to give 6 module passes. In a working system, a heat transfer fluid passes through the modules to provide or remove heat during ammonia adsorption or desorption. The reactor was loaded with 97 kg (213 lb) of the pure salt needed for forming the complex compound, CC180-1580.

The first ammoniation was performed with the reactor cooled by water recirculated from a water reservoir at 43°C (110°F). Ammonia cylinders placed in the reservoir were used to provide ammonia to the reactor. During ammoniation, heat was removed from the reservoir by the vaporizing ammonia in the cylinders, and added to the reservoir by the exothermic adsorption reaction which took place in reactor. Thus, the water reservoir served as a thermal buffer for the ammonia supply cylinders and the reactor assembly. Ammoniation proceeded for approximately 2 h, and 80 kg (175 lb) of ammonia were adsorbed as determined from the initial and final weights of the ammonia cylinders. This quantity of ammonia corresponds to 7.7 moles of ammonia per mole of salt which was the expected saturation level.

Following this conditioning cycle, adsorption testing to determine ammonia uptake rates and capacity were performed with the reactor at 16°C (60°F) nominal temperature and ammonia vapor pressure of 9.5×10^{-4} Pa (0.95 atm) corresponding to an ammonia evaporator pressure of -34°C (-30°F). Adsorption was performed using the procedure for the first ammoniation. The results from this adsorption are shown in Fig. 1. The rates shown were measured by an ammonia mass flow meter located between the ammonia supply cylinders and the reactor. One curve shows the instantaneous rates, a second curve shows rates averaged over several minutes, and the third curve shows the rates as determined by the enthalpy change of the cooling water provided to the reactor. The average adsorption rate as determined by these measurements remained over 2 mol/mol-h for the entire period. This is an important finding since in a typical chill TES application, a 4-h on-peak period would require an adsorption rate of at least 1.5 mol/mol-h.

Desorption tests were also conducted, but experimental difficulties combined with the absence of a compressor with a capacity large enough to generate meaningful results prevented an accurate determination of the desorption performance of the system. Further

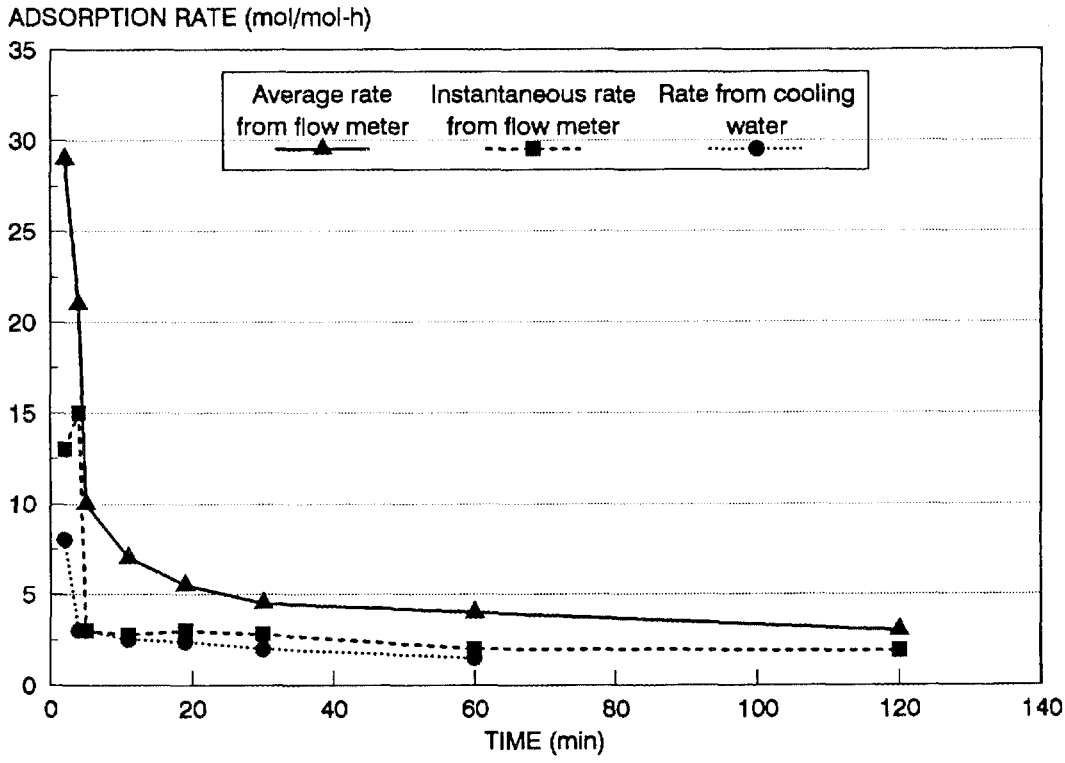

Fig. 1. Ammonia adsorption rate in 4 ton-h reactor.

work to determine the desorption performance was continued.

The conclusions thus far in the project support the contention that complex compound chill TES systems are technically viable and may be economically attractive. It was demonstrated that functional reactors could be assembled in a factory environment, and they perform as well as smaller laboratory systems studied earlier. Future work will concentrate on identification, performance verification and optimization of the internal heat exchanger to improve system cost-effectiveness, and field operation and testing of the optimum exchanger surface.

2.2 DIRECT CONTACT ICE SYSTEM DEVELOPMENT

The objective of this project was to design, build and test a direct contact ice storage system for electric load management of building air conditioning loads and to compare this performance with currently-available ice storage systems. To accomplish this task, a prototype 88 kW, 3.8 GJ (25-ton, 300 ton-h) system was designed, built and tested by CBI. The

prototype tests were structured to determine the production, storage and discharge characteristics of the direct contact ice system and to determine component performance during charging (ice making) and discharging (ice melting) operations.

2.2.1 System Description and Operation

The CBI system, shown schematically in Fig. 2 makes ice by direct contact between the evaporating refrigerant and water. The refrigerant R-114 and water are sparged together in four direct contact evaporator freezers F1 through F4 located in the vapor space of the ice storage tank, T1. As the ice particles form, they fall from the freezers into tank T1 for

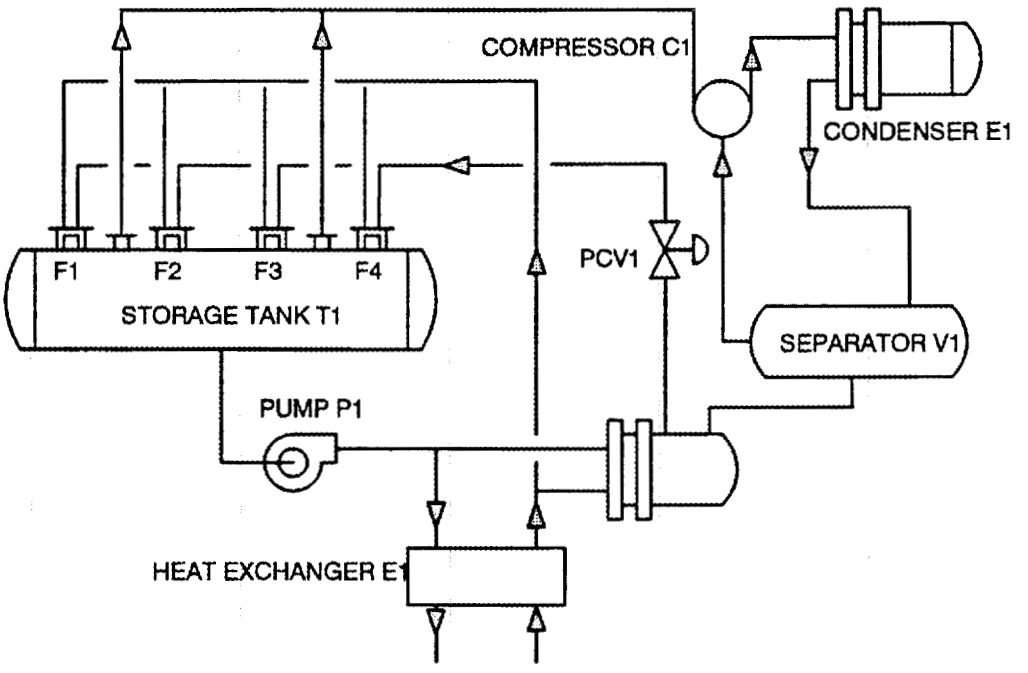

Fig. 2. Schematic of direct contact ice maker.

storage. This tank was 2.4 m (8 ft) in diameter and 5.2 m (17 ft) long and was sized to meet the 300 ton-h ice storage capacity required. During charging, the cold water pump (P1) circulates water from the tank to the evaporators where ice is formed by direct contact with vaporizing R-114. The plate frame heat exchanger is used during the discharge (ice melting)

mode to meet the building cooling load that was simulated in these tests. The unique feature of the system is the liquid ring compressor, a rotary displacement pump which uses water to seal and lubricate the rotor vanes. During operation, some of this seal water and all of the compressed refrigerant gas are discharged to the condenser (E1) where the refrigerant condenses and drains along with the seal water into the refrigerant/water separator vessel (V1). Seal water is returned to the compressor suction by the overpressure in this separator. The compressor capacity was expected to vary with seal water flow rate; consequently, the test plan required the compressor to be operated at various seal water flow rates to determine the effect of seal water flow rate on overall system efficiency and to determine the optimum seal water flow rate. The condenser is a conventional single wall tube-in-tube heat exchanger with refrigerant on the outside and cooling water on the inside. The refrigerant/water separator vessel (V1) is a 0.4-m (16-in.)-dia. by 1.0-m (40-in.)-long cylindrically shaped horizontal tank. This separator operates at a pressure of about 2.4×10^5 Pa (35 psia), and the ice tank operates at about 7.6×10^4 Pa (11.0 psia) so that refrigerant is returned to the freezers due to the difference in these pressures. The refrigerant flow rate is controlled by pressure control value PCV1 which is actuated by the tank operating pressure.

2.2.2 Instrumentation

Pressures, temperatures, flow rates, and electrical energy use of the various components of the system were measured to determine system performance. If was found that the ice fraction is directly proportional to the concentration of salt ions (and therefore the electrical conductivity) in the water so that a conductivity probe could be successfully used to determine the ice inventory. A correlation between the electrical conductivity and the salt concentration was used to calculate the amount of ice as a weight fraction of the tank contents.

2.2.3 Test Procedure

The procedure during the charging mode was designed to determine the system power consumption, ice production rate and the rate of refrigerant carryover into the storage tank during operation. The two major consumers of electrical energy were the refrigerant

compressor (C1) and the recirculation pump (P1). Although the power consumption of the pump does not vary appreciably since the recirculation flow rate is relatively constant, the capacity and power consumption of the compressor were affected by the compression ratio and seal water flow rate. Since the tank pressure is virtually constant, the compression ratio could be varied only by changing the condensing pressure. This was accomplished by controlling the condenser water flow rate.

The compressor performance was also affected by the seal water flow rate. Higher seal water flow rates corresponded to increased compressor capacity. In the charging tests, the seal water flow rate was varied between 4.4×10^{-4} and 6.3×10^{-4} m^3/s (7.0 and 10.0 gal/min) to determine its effect on capacity, compressor power and overall system efficiency.

The performance (ice production rate) of the direct contact freezers (the ice production rate) was determined by calculating the evaporator capacity from the flow rates of water and refrigerant to the freezers and the temperature difference between them. The rate of refrigerant carry-over into the ice storage tank was determined by monitoring the refrigerant level in vessel V1 at regular intervals during charging. Water carry-over from the ice storage tank into the separator was also recorded.

The test procedure during the discharging mode was designed to determine the effect of ice melting rate on supply and return water temperatures to the storage tank. The discharge rate was varied by manually controlling the flow rate of warm water from a large heated tank through heat exchanger E1.

Measurements of compressor power were conducted with electrical power transmitters appropriately corrected for motor efficiency. Condenser heat rejection was calculated from the temperature rise and flow rate of the condenser water, and the delivered cooling during discharge was calculated from the coolant flow rate and temperature rise across the storage tank.

Three methods were employed to determine the cool stored in the tank during charging. The first method assumed a global heat balance on the system and assumed that cooling provided to the storage tank was the difference between the energy provided to the compressor and the heat rejected by the condenser. The second method used the conductivity probe in the storage tank to determine the amount of ice formed as a function of charging time. The third method assumed that the heat added to the tank during discharge (ice melting) was equal to the heat removed from the tank to make ice during the previous

charging period. In this method, heat gains to the tank from ambient were not considered. During the testing phase, the charging capacity as determined by each of these methods agreed to within ±10%.

2.2.4 System Performance

The direct contact ice storage system was operated for more than 500 h; more than half of this time was for ice making and the remainder for ice melting. Operating the system on an uninterrupted basis showed that the system was reliable and generally trouble free requiring no operator intervention. Maintaining a constant evaporator pressure was simple even when the tank pressure controller was operated manually. Although ice tended to pile up under the freezers, the freezers continued making ice. A small amount of refrigerant was carried over into the ice storage tank from the refrigerant/seal-water separator during charging operation, but this was easily recovered at the beginning of a subsequent run.

2.2.4.1 Charging performance

Charging performance was determined according to the test schedule given in Table 1. The values in this table are averages for the duration of each test. The condensing pressure and compressor seal water flow rate were changed for each test. Since the freezers are located inside the ice storage tank, the evaporating pressure and ice storage tank pressure are equal and are maintained at the desired set point by controlling the refrigerant flow rate into the freezers through control valve PCV1 shown in Fig. 2. The benefits of a high control valve setting are (1) an increase in refrigerant flow rate to the freezers, and (2) a reduction in pressure drop through the control valve thereby providing high pressures at the inlet to the freezers. Tests at higher condensing pressures resulted in higher pressures at the inlet to the freezers. However, higher compression ratios reduced the compressor capacity so that the control valve was throttled to maintain ice storage tank pressures. As Table 1 indicates, a fully open control valve produced the highest capacity and lowest energy consumption. Tests showed that raising the seal water flow rate increased the refrigerant compressor capacity. From run 5 to run 8, the control valve was 100% open, and the seal water flow rate was varied from 7.0 to 10 gal/min.

Table 1. Summary of direct contact ice making tests

Run no.	Seal water flow rate (gal/min)	Control valve opening (%)[(A)]	Capacity (ton)	Compressor power (hp)	Energy consumption (kW/ton)	Final ice fraction (%)[(B)]
1	8.0	43	10.5	47.7	3.4	33
2	6.5	48	10.5	46.5	3.3	35
3	6.8	66	11.2	46.5	3.1	30
4	7.1	80	11.8	47.0	3.0	52
5	8.0	100	12.5	48.1	2.9	49
6	9.1	100	13.2	49.5	2.9	52
7	7.1	100	12.0	47.7	3.0	46
8	10.0	100	13.3	51.2	2.9	40
9	9.3	59	12.2	50.8	3.2	21

(A) Percent that PCV1 is open
(B) Percent of H_2O in storage tank that is ice

The effects of seal water flow rate on energy consumption, capacity and compressor power are shown in Fig. 3. These data show that as the seal water flow rate increases from 7 to 10 gal/min, the capacity increases at a faster rate than the power consumption so that the efficiency of the system improves. Data for seal water flow rates above 10 gal/min could not be produced without overloading the compressor motor drive. The energy consumption varied between 2.8 and 3.4 kW/ton. This is high compared to measured energy consumptions of conventional ice storage systems[4]. The low efficiency for the direct contact system is due to the poor efficiency of the liquid ring compressor (calculated to be approximately 30%).

2.2.4.2 Discharging performance

After each charging test, the tank was discharged until all the ice was melted. A summary of the discharge test results is shown in Table 2, and the tank leaving water

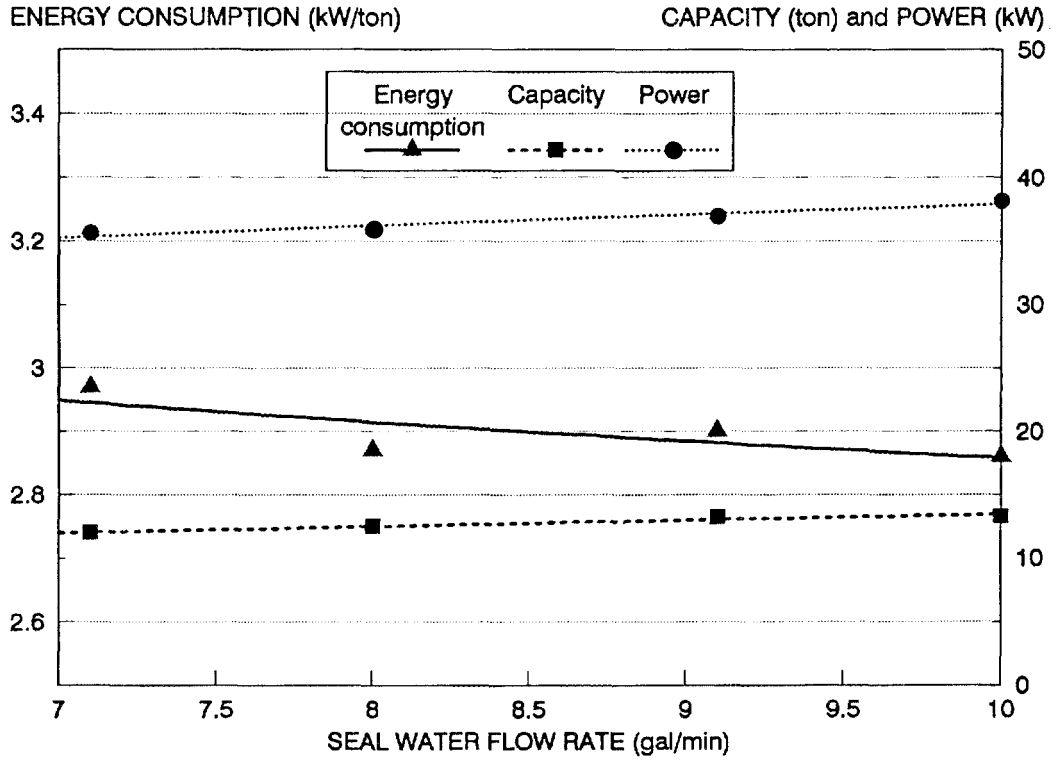

Fig. 3. Direct contact ice making performance.

temperature from a typical discharge test is shown in Fig. 4. The discharge capacity was maintained relatively constant during each test by controlling the temperature difference across the discharge heat exchanger (E2) and maintaining a constant flow rate. As can be seen in Fig. 4, the initial supply water temperature was 0°C (32°F) and as discharge continued, remained below 3.2°C (40°F) until the design capacity of the storage tank was reached. This discharge performance is typical for conventional dynamic ice makers that shuck ice into a bin for storage. The capacity and temperature values listed in Table 2 are averages for each test, and the total storage capacity (the last column in this table) is taken to be the cumulative capacity with a maximum supply water temperature of 40°F. It was noted by CBI that colder supply water temperatures could have been maintained if agitation has been used in the ice storage tank or a more effective cold water piping configuration had been used in the tank.

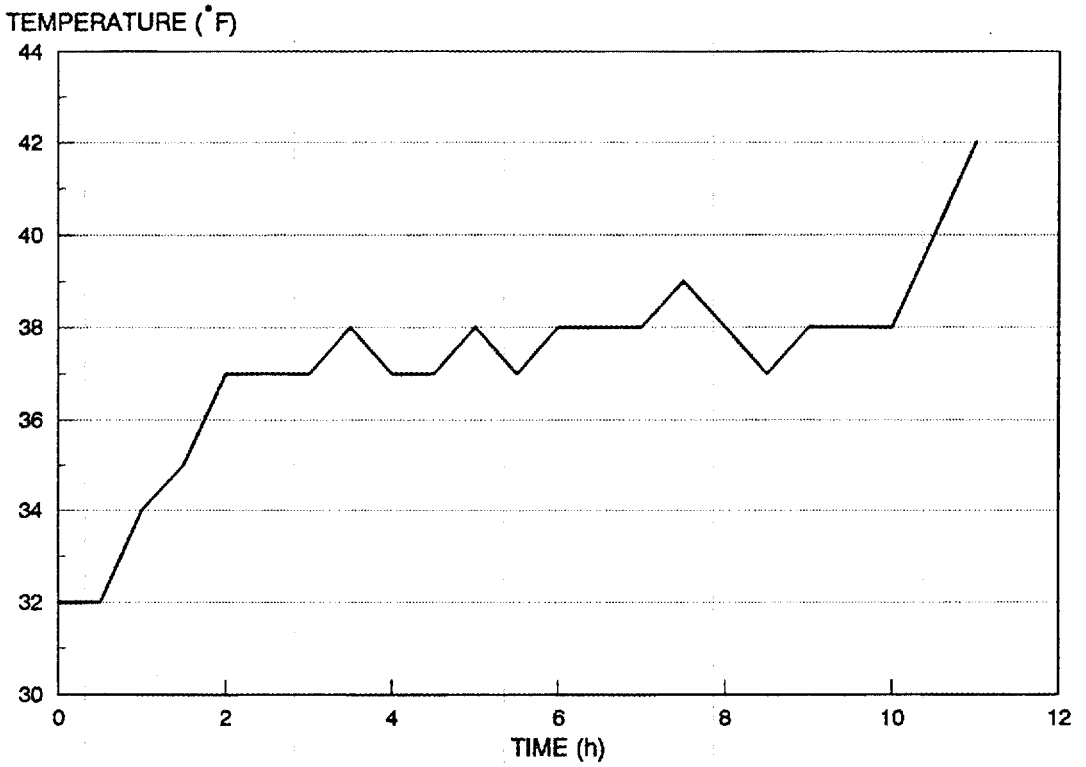

Fig. 4. Tank leaving water temperatures during melting.

2.2.4.3 Equipment Performance

The freezers did not plug and a constant evaporating temperature of approximately -2°C (28°F) was maintained during the operating period. This evaporator temperature is several degrees higher than measured evaporator temperatures from conventional ice makers.[4] During charging, the ice storage tank operating pressure was less than atmospheric; however, it was found that very little purging of noncondensibles was required. The major problem experienced was ice buildup from the bottom of the tank to the freezers, and it was felt that this problem could be solved with better attention to freezer location inside the tank. Prior to test initiation, corrosion coupons were installed in the vapor space and liquid region of the storage tank to determine the potential for corrosion with the R-114/water mixture. Although the test period was relatively short, posttest inspection of these coupons showed no evidence of corrosion.

Table 2. Summary of ice melting tests

Run No.	Starting ice fraction (%)	Supply temperature (°F)	Return temperature (°F)	Melt time (h)	Discharge capacity (ton)	Total storage capacity (ton-h)
1	31	36.0	40.7	9.3	26.1	243
2	34	35.0	38.6	10.8	19.9	216
3	28	35.7	41.0	6.3	31.0	196
4	51	36.0	40.1	13.6	22.5	306
5	48	37.1	42.0	10.6	28.6	303
6	52	37.0	41.6	9.2	33.2	204
7	46	38.0	44.3	7.5	36.5	274
8	38	34.7	37.7	15.0	14.8	222

In summary, although the evaporator temperature during ice making was high which would otherwise tend to improve ice-making efficiencies, the overall system efficiency was lower than expected and lower than measured efficiencies of conventional ice storage systems. Identification of a suitable compressor technology with higher efficiency is required to improve the overall performance of the system. A second major issue is the fact that the CBI system is based on R-114, a refrigerant which is being phased out due to its detrimental impact on atmospheric ozone. Further work with this direct contact concept will depend on the identification of an acceptable alternative refrigerant.

2.3 PCM WALLBOARD DEVELOPMENT

Work was continued in the development of building materials with enhanced heat capacity. Prior work showed that paraffin blends can be used as room temperature PCMs and can be incorporated into plasterboard up to 33 wt. % of composite. Research during the reporting period characterized the fire safety of such a system and examined methods for

amelioration of this problem. In addition, methods for adding the PCM to the wet mix during plasterboard manufacture were studied, and modifications were made to a PCM wallboard simulation code that allow the PCM to melt and freeze over a small temperature range rather than at a single temperature.

2.3.1 PCM Wallboard Fire Safety Studies

Experiments were conducted to improve the fire safety and flame spread characteristics of the PCM wallboard by (1) reducing the quantity of PCM, (2) using chemical fire retardants, and (3) using coatings to prevent wicking of the PCM to the plasterboard surface.

2.3.1.1 Reduced Levels of PCM

The major component in plasterboard is gypsum ($CaSO_4 \cdot 2H_2O$) which does not burn. It was found that imbibing the plasterboard up to the full limit of 33% of PCM makes it flammable as measured by a horizontal flame test conducted in the laboratory. It is possible and has been demonstrated in the full scale that by varying the time of immersion of the plasterboard in molted PCM, the uptake of PCM can easily and accurately be controlled. The PCM can also be diluted with a solvent such as methylene chloride to reduce its concentration still further. A series of samples varying in PCM content from 2 to 23 wt. % were prepared and tested for flammability. The samples containing 18% PCM self-extinguished in 5 s and lower concentrations extinguished even faster.

2.3.1.2 PCM Wallboard Covered with a Nonflammable Surface

Since PCM plasterboard burns along the paper surfaces as the paraffin wicks to the surface, it was anticipated that application of a nonburning surface such as aluminum would protect the paper and prevent the paper from burning. A generally accepted method for testing fire spread characteristics of materials is ASTM E-84 which requires a Steiner tunnel. In this tunnel, the sample to be tested is installed as the ceiling and the walls and floor are of nonflammable materials. A calibrated flame is started at one end of the tunnel, and the

progression of the flame along the tunnel is monitored in terms of distance along the tunnel and time. The area under this distance-time curve is a measure of the flame spread behavior of the material tested. A Steiner tunnel was made available by National Gypsum Company (NGC) to the PCM wallboard project, and samples of aluminized PCM wallboard were prepared and tested for flame propagation. These tests showed that the aluminum foil quickly melted at the high temperatures in the tunnel and increased the level of smoke generation. The results of these tests also showed that the flame spread index of the PCM plasterboard covered with aluminum foil was equal to that of a common hardwood (red oak), but the index for smoke generation was much higher that for the wood. Visual smoldering of the surface was also reported.

2.3.1.3 Flame Suppression using Fire Retardants

Chlorowax 70S and antimony pentoxide, the cheapest and most common fire retardants, are insoluble in the paraffin PCM and therefore could not be used in sample preparation by immersion. Several halogenated organic compounds were examined and Ethyl Corporation's BCL-462 was found to be soluble with paraffin in all proportions. Plasterboard samples prepared with Witco 45A, the PCM blend most favored, and BCL-462 in the ratio of 75/25 were shown in laboratory tests to have improved fire retardance; however, increased levels of smoke generation were noted. Similar results were also obtained using Ferro Chemical Company's Bromochlor 70 as a fire retardant. Attempts were made to introduce a blend of the BCL-462 and submicron particle size antimony pentoxide into PCM plasterboard samples. The results of this effort showed that the chemicals could not be evenly distributed in the treated plasterboard as evidenced by the presence of antimony pentoxide only on the surface of the boards rather than permeated throughout.

Efforts were initiated to capitalize on the observation that plasterboard burning consumes the paper rather than the core of the material, and tests of fire retardants applied to the front and back surfaces of wallboard were conducted. Using this approach, a posttreatment of PCM wallboard with fire retardant chemicals was anticipated to improve the safety of the building material. To test this hypothesis, PCM wallboard samples with a surface treatment of Dow Chemical's Fyrol CEF (trichloroethyl phosphate) was prepared and tested for flame spread and smoke development in the Steiner tunnel. Results from these tests are

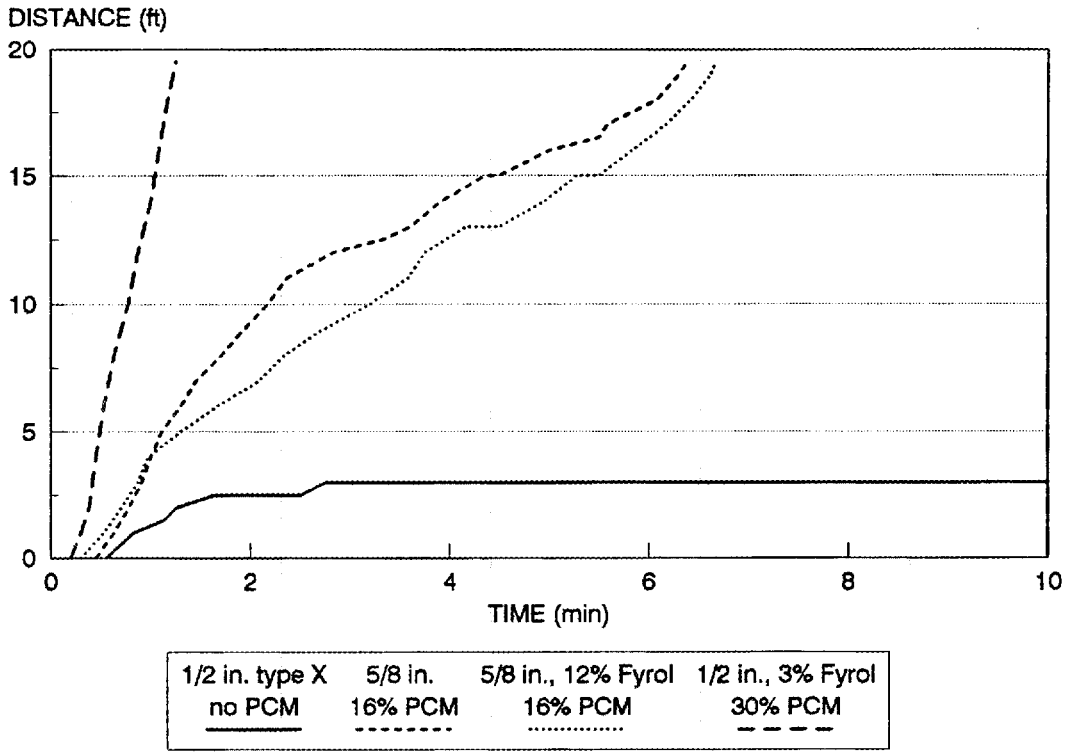

Fig. 5. Steiner tunnel test results of PCM wallboard.

shown in Fig. 5. In test 1, a control sample of 1/2-in. type X gypsum wallboard was used. Test 2 used 5/8-in. wallboard containing 16 wt. % PCM. Test 3 used 5.8-in. wallboard containing 16 wt.% PCM and Fyrol CEF. Test 4 used 1/2-in. wallboard containing 30 wt. % PCM and Fyrol CEF. As can be seen from tests 2 and 3, the Fyrol was somewhat effective in reducing the flame spread characteristics of the wallboard; however, the smoke development worsened. The results of test 4 show that the 1/2-in. sample with 30% PCM and Fyrol is very combustible; further, the combustibility would be still greater without the Fyrol. This assertion is based on a comparison between tests 2 and 3. The results from these tests and follow-up discussions with NGC indicated that (1) wallboard with high PCM concentrations would be unacceptable, (2) additional testing should be done at concentrations less than 16%, and (3) increased attention should be devoted to identifying fire retardant systems better suited to the application.

2.3.2 Alternatives to PCM Imbibing Process

Plasterboard manufacturers including NGC and USG have noted that the availability of a PCM as a solid powder that could be added to the wet mix during plasterboard manufacture would be more attractive than the imbibing process since virtually no changes to the manufacturing process would be needed. The paraffin PCM cannot be added directly to the wet mix because it liquifies below the plasterboard formation temperature thereby reducing the strength of the manufactured panels. Responding to this interest, the UDRI under the TES program examined mixtures of the paraffin PCM and various silicas that together produce a dry powder that can be added to the wet plasterboard mix. It was found that a free flowing powder containing up to 75% by composite weight of the paraffin PCM could be obtained by this method. Mixtures of hydrophilic silica (Cab-O-Sil MS-7) and the PCM were found to phase separate in the wet mix of plaster and release the PCM which is hydrophobic. Experiments showed that hydrophobic silicas (Cabot TS610, Degussa R972) should not absorb water and should retain the hydrophobic PCM much better.

To test this hypothesis, mixtures of approximately 20% and 30% PCM contained in a matrix of three silicas (Cab-O-Sil MS-7, Cabot TS610 and Degussa R972) were chosen for experimental study. The control samples were the three silicas containing 20% and 30% water instead of the PCM. Batches of three cubes from each silica/PCM mix and controls were made and used for the following process studies: water absorption compressive strength, and thermal energy storage capacity as determined by DSC. The water absorption characteristics of these samples shown in Table 3 indicate that all of the samples absorbed water readily and could be dried. However, the hydrophobic silica samples with PCM picked up less water and lost less weight on drying. This is important since much of the manufacturing cost of plasterboard is associated with a drying operation to remove excess moisture.

Samples were subjected to compression testing, and the strengths of samples with Cab-O-Sil MS-7 or a combination of Cab-O-Sil MS-7 and the PCM were found to be equal to or better than the control samples with none of these ingredients. Cubes with a combination of hydrophobic silica and the PCM also had compressive strengths equal to that of the controls.

Table 3. Water pick-up of plaster cubes (USG) with hydrophilic silica/PCM and hydrophobic silica/PCM

Sample	Initial wt. (g)	Soaked in water overnight (g)	% Pickup	After drying 1 week (g)
Control No PCM No Silica	75.73	121.40	60.31	71.24
Cab-O-Sil MS-7[(A)] Control (20%)	84.70	141.48	67.04	82.84
Cab-O-Sil MS-7[(A)] Control (30%)	79.59	137.21	72.40	77.77
Cab-O-Sil MS-7[(A)] 20% PCM	99.72	150.78	51.20	99.03
DeGussa R972[(B)] 20% PCM	112.22	163.06	45.30	111.66
DeGussa R972[(B)] 30% PCM	112.20	154.03	37.28	111.53
Cabot TS610[(B)] 20% PCM	111.04	156.55	40.99	110.55
Cabot TS610[(B)] 30% PCM	113.20	152.72	34.91	112.77

[(A)]Hydrophilic silica
[(B)]Hydrophobic silica

Heat capacities of PCM/silica samples were measured by DSC at heating and cooling rates of 2° C/min and 10° C/min. In the case of hydrophilic silica, the DSC showed that the

melting peak was unaffected, but the crystallization peak showed several discontinuities possibly due to absorption and desorption of PCM at the surface of the silica. The DSC also showed that the presence of hydrophilic silica in the PCM gave rise to an additional (minor) solid-state transition at temperatures lower than the melt temperature. It has been suggested that the lower temperature peak is due to the treatment of the silica to impart hydrophobicity.

2.3.3. PCM Wallboard Computer Simulation and Validation

A numerical code, WALL88 initially developed by ORNL in 1988 to study the thermal response of buildings with PCMs, was exercised to characterize the transient thermal transport and storage of sensible and latent heat in multicomponent building materials such as the PCM wallboard.[5] The code treats the PCM via two methods: (1) as uniformly mixed with the matrix material, and (2) present as discrete 2-D PCM pellets distributed randomly throughout the solid support matrix. The code allows one to select the method to be used. Surface boundary conditions allow convective heat transfer the room air as well as direct gain of solar energy. The full mathematical foundation for the code was developed in earlier studies.[6] Efforts during the current reporting period consisted of experimental confirmation of the model for both sensible and latent heat storage tests.

An unguarded thin heater apparatus (UTHA) was used to determine the conductivity of PCM wallboard samples and to determine the transient response of these materials with a step change in flux on one surface of the wallboard and the second surface remaining isothermal. Fig. 6 shows a side-view schematic of the UTHA and defines the surface temperature locations. At time equal to zero the resistance heater is turned on, but the cold plates continue to maintain the upper and lower surface temperatures of the plasterboard samples constant. The initial temperature in this experiment is 26.5°C (79.7°F), which is above the melting point [23.0°C (73.5°F)] of the paraffin in the plasterboard. Therefore, sensible heat is the only thermal storage mechanism involved. By knowing the heat flux from the resistance heater, the temperature difference between the heater and the cold plate, and the thickness of the stack of four plasterboard samples, the overall thermal conductivity was calculated.

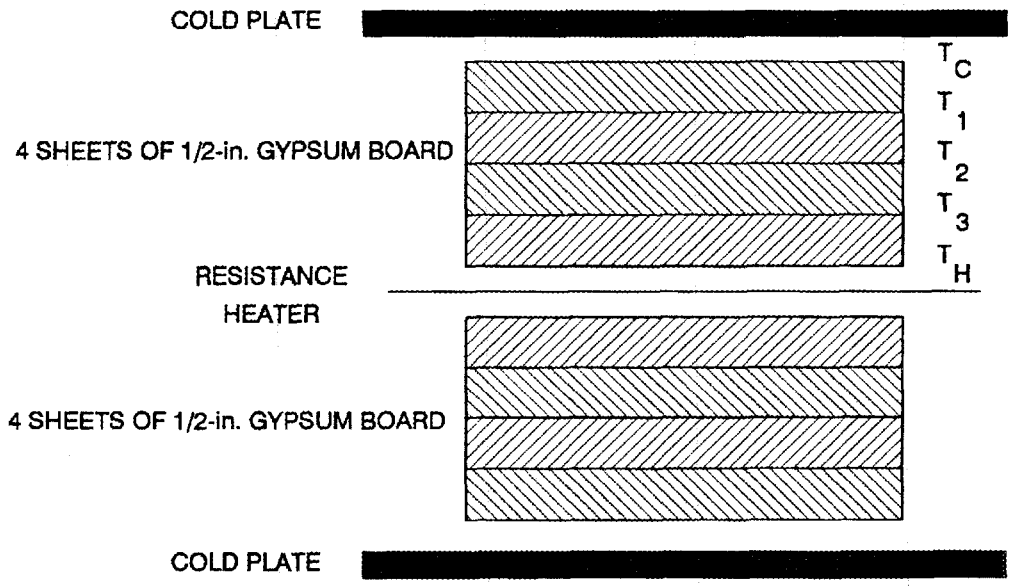

Fig. 6. PCM wallboard testing in the UTHA.

Based on the experimentally-determined conductivity, the computer code was used to predict the transient in terms of plasterboard interface temperatures. The results of these predictions and interface temperatures measured in the UTHA are shown in Fig. 7. The agreement between measured and computed temperature values is very good for temperature locations T_H and T_3 but deviates for temperature locations T_1 and T_2. The good agreement between experiment and predictions for T_H and T_3 was due to using a value for wallboard conductivity at these temperatures. If the thermal conductivity was computed based on the measured temperature difference between T_C and T_1, then the computed and measured values of T_1 were found to be in good agreement; however, the predictions of T_H would be inaccurate. Based on these results, it was concluded that the ability of WALL88 to describe accurately sensible heat transients was verified.

The capability of WALL88 to predict temperatures in the case of latent heat was verified by comparing its predictions to a known analytical solution.[7] The configuration for which a closed solution is known is a semi-infinite volume of immobile liquid at its melting point. At time equal to zero, the surface of the semi-infinite solid is fixed at a temperature

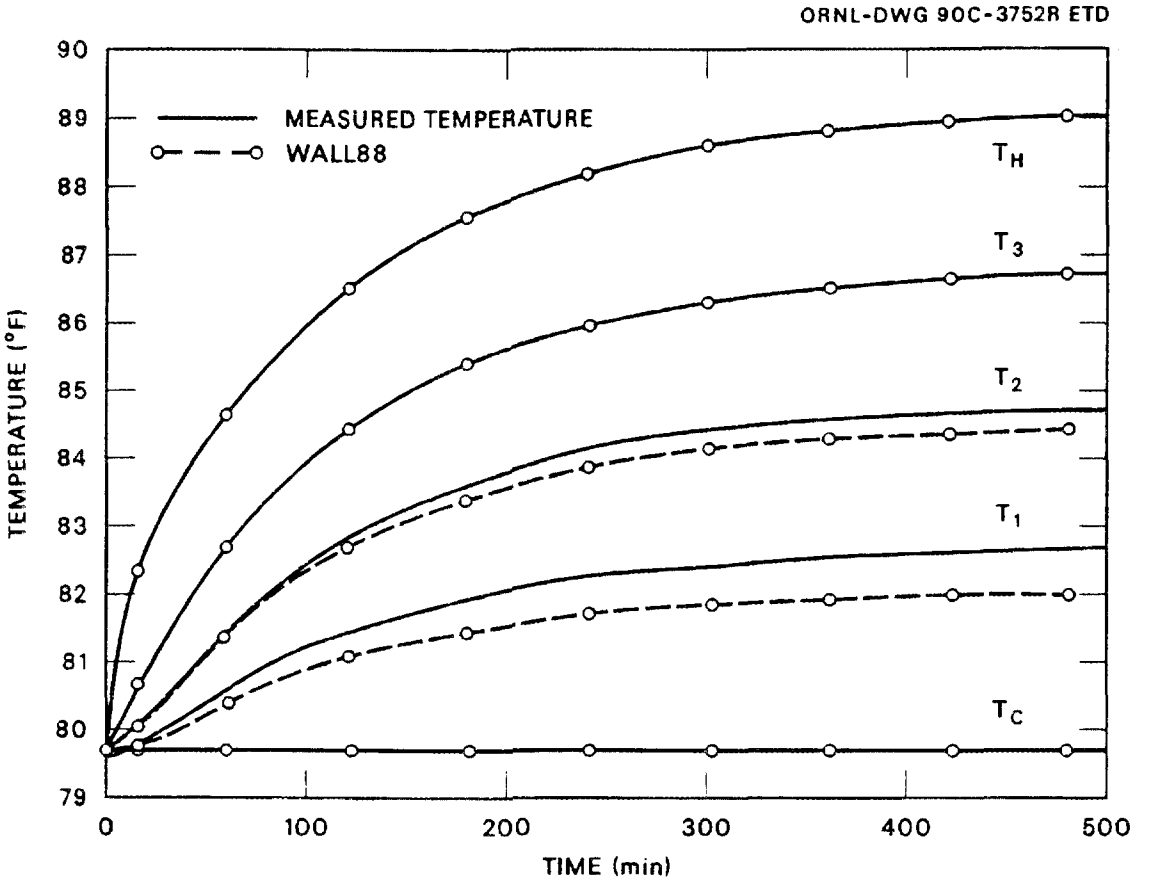

Fig. 7. Comparison of WALL88 with experimental transient.

below the melting point, and the liquid starts to freeze. The closed form equation relates the temperature in the solid phase to distance and time. For this verification example, the initial liquid temperature was -6.7°C (20°F), which was also the fictitious solid's melting point. At time equal to zero, the surface was fixed at -17.8°C (0°F). Other parameters were heat capacity = 1.47 kJ/kg·°C (0.35 Btu/lb·°F), conductivity = 0.835 kJ/h·m·°C (0.134 Btu/h·ft·°F), density = 1.0 g/cm³ (62.4 lb/ft³), and heat of fusion = 58.8 kJ/kg (25.3 Btu/lb). The temperature profile in the solid was computed after 4 h, and the results are shown in Fig. 8. The agreement is quite good, and it was concluded that the ability of WALL88 to predict temperature response for this limiting case was verified.

Further studies to validate WALL88 with an experimentally produced transient were also conducted. In this case, the transient with plasterboard containing 30% paraffin was repeated. For this test, the initial temperature was 22.5°C (72.5°F), which is below the melting point of 23.0°C (73.5°F). The experimental data from this transient are shown in

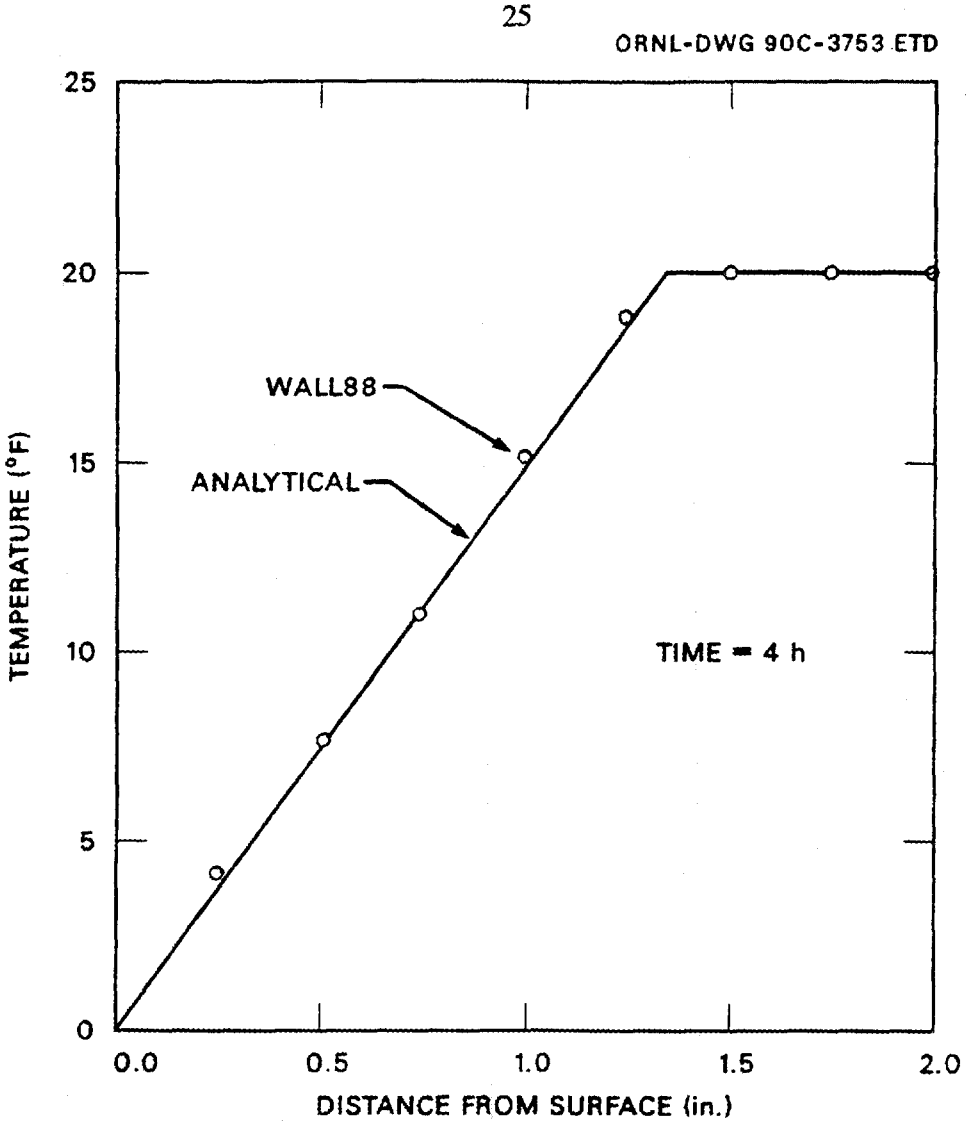

Fig. 8. Comparison of WALL88 to known analytical solution.

Fig. 9. The entire transient lasted about 4500 min, or 3 days. With the heater power set as before, the duration of this transient was tenfold that shown for the sensible only transient in Fig. 9—clear evidence of the benefit of latent heat as an energy storage mechanism. Also indicated in Fig. 9 are the results of a WALL88 simulation with the following property data:

Melting point = 23.3°C (74.0°F)

Paraffin concentration = 30 wt. %

Heat of fusion = (30%)(195.2 kJ/kg-paraffin) = 58.6 kJ/kg (25.2 Btu/lb)

Heat capacity = 1.47 kJ/kg·°C (0.35 Btu/lb·°F)

Thermal conductivity = 0.835 kJ/h·m°·°C (0.134 Btu/h·ft·°F).

ORNL-DWG 90C-3754R ETD

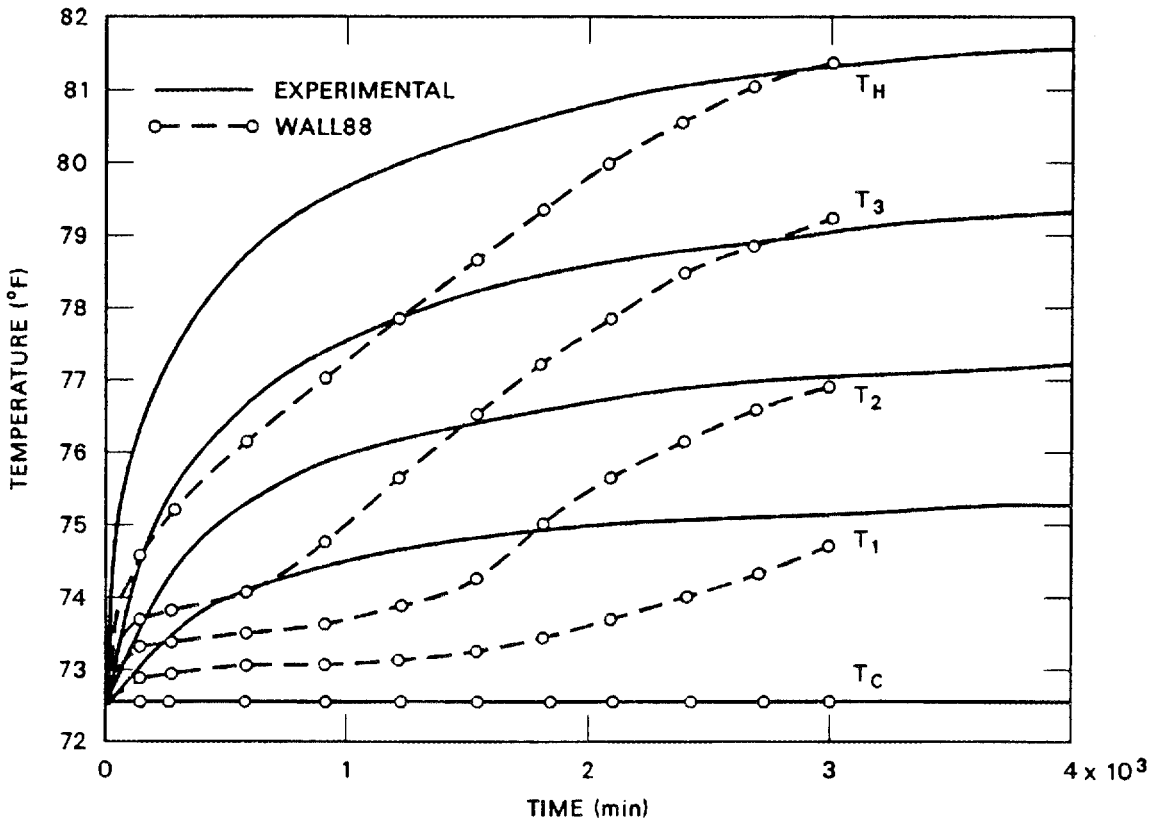

Fig. 9. Comparison of WALL88 to experimental transient data. Assumed melting point: 74°F.

The measured and computed temperatures did not agree; the computed temperatures tended to level off at the melting point whereas the measured temperatures did not. A series of additional simulations in which the property data were modified somewhat failed to produce agreement between model and measurement.

To improve agreement between the two, the model was modified to allow the paraffin to melt over a range of temperatures. This change was made to reflect the melting curve of the PCM as determined by DSC and shown in Fig. 10. It can be seen that the PCM melts over a range of about 5.5°C (10°F) which approximates the temperature range determined in the transient experiments. Therefore, WALL88 was modified to incorporate a melting range in which the heat of fusion was replaced by the triangular heat capacity relationship shown in Fig. 11. The points TA, TB and TM represent the onset of melting, the end of melting and the "midpoint" of melting, respectively. These temperatures are shown in Fig. 11: TA is the temperature at which the melting curve first becomes apparent [22.0°C

ORNL-DWG 90C-3750 ETD

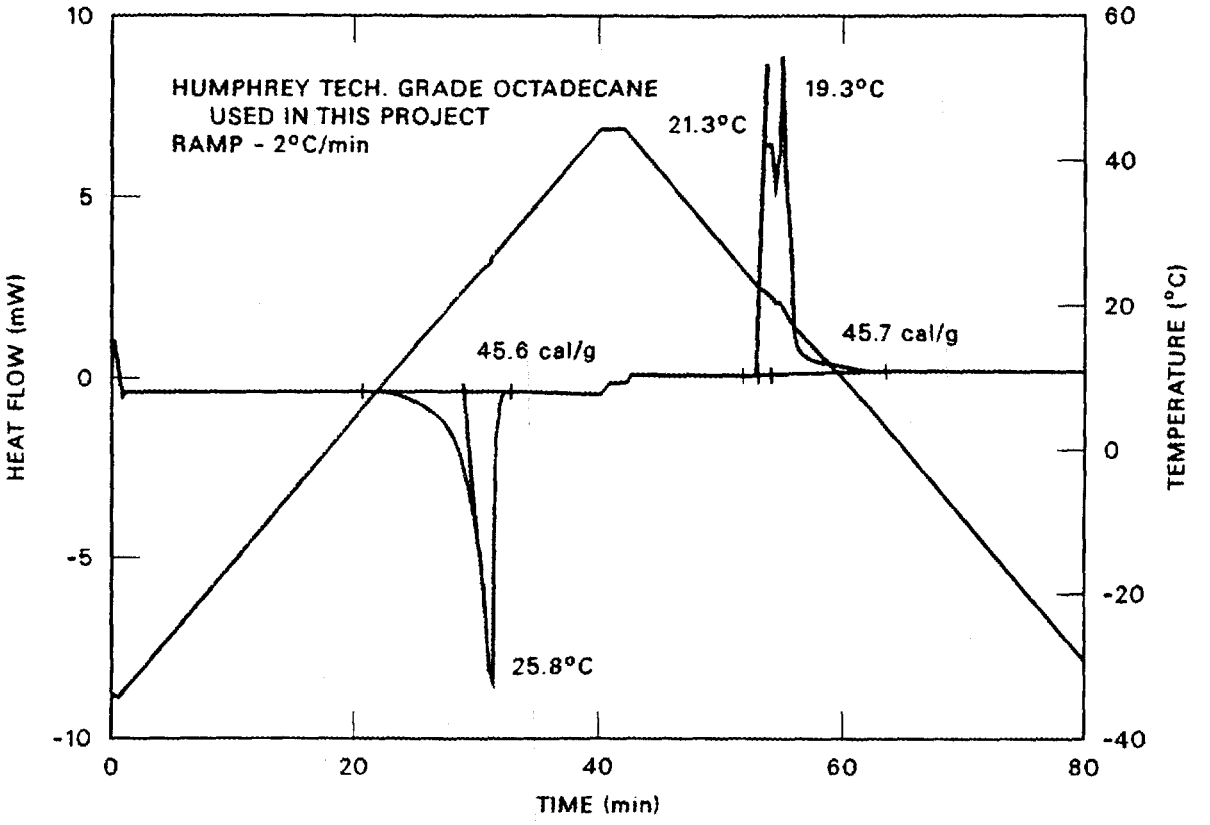

Fig. 10. DSC plot for the paraffin blend used in this project.

(71.6°F)]; TM is the melting peak [25.8°C (78.5°F)], and TB is the temperature at which the melting curve rejoins the sensible heating ramp [28.0°C (82.4°F)]. The heat of fusion measured by DSC was apportioned to represent the shaded area in Fig. 11, yielding a Cp-MAX of 15.2 kJ/kg·°C (3.62 Btu/lb·°F). The results of a simulation using these changes shows marked improvement as indicated in Fig. 12.

It was concluded that the paraffin does indeed melt over a temperature range as determined by the DSC rather than at a single temperature as an idealized PCM, and the simulation should be designed to accommodate this melting range. Further, values for the heat of fusion, "onset of melting" and "end of melting" temperatures as measured by the DSC and used in the model improve the agreement between simulated and actual transient temperature response. Further work is underway to describe the thermal behavior of PCM plasterboard samples as the PCM freezes.

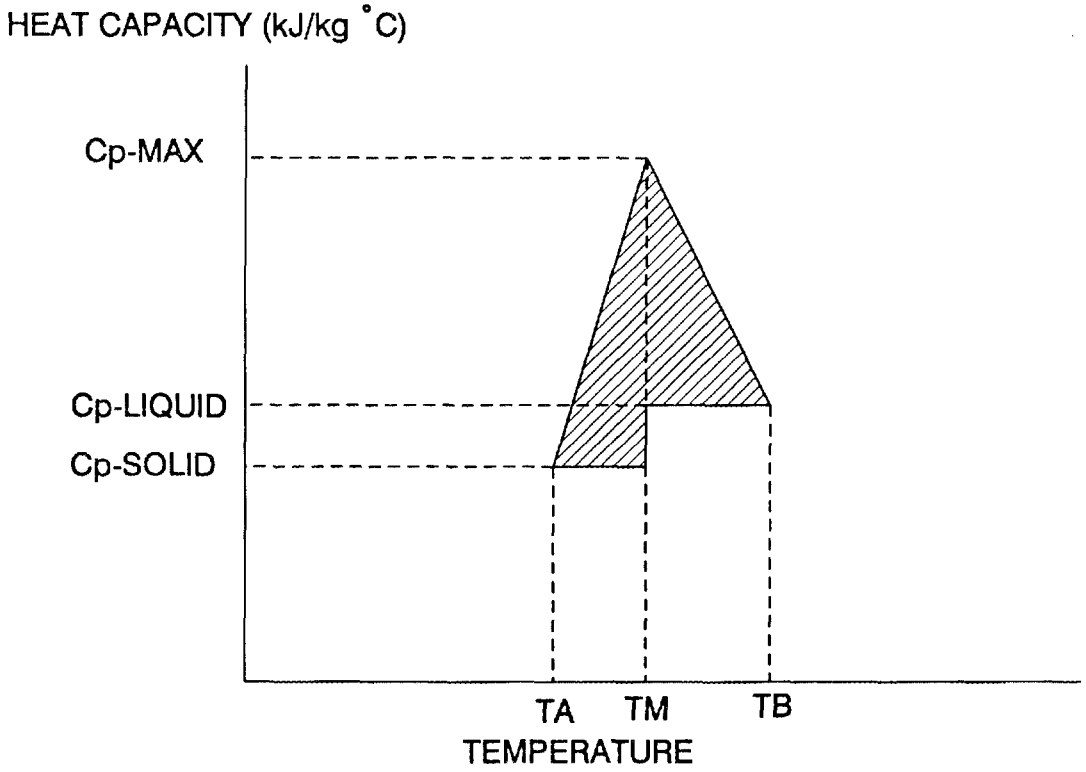

Fig. 11. Heat capacity relation to simulate a melting range.

2.4 EFFECT OF DOPANTS ON SOLID-STATE PCMS

The overall objective of this project was to determine phase transition mechanisms in organic TES materials in which the heat is reversibly absorbed during solid-solid phase transitions. Pure organic polyalcohols ("plastic crystals") undergo crystallographic changes absorbing or releasing large amounts of latent heat at constant transition temperature well below their melting points. There are relatively few known pure polyalcohols which undergo solid-solid phase transitions storing latent heat, and most of these have high transition temperatures. Lowering these transition temperatures while retaining a significant portion of the latent heat is important for development of practical TES materials. In this project conducted by the University of Nevada - Reno, binary polyalcohol compounds were studied to adjust transitions to near room temperature. In this project, the crystallographic changes of several polyalcohols with the addition of a second component or dopant was determined. These polyalcohols were: pentaerythritol (PE), pentaglycerine (PG), neopentylglycol (NPG), trimethylol propane (TMP) and 2-amino 2-methyl 1,3 propanediol (AMPL).

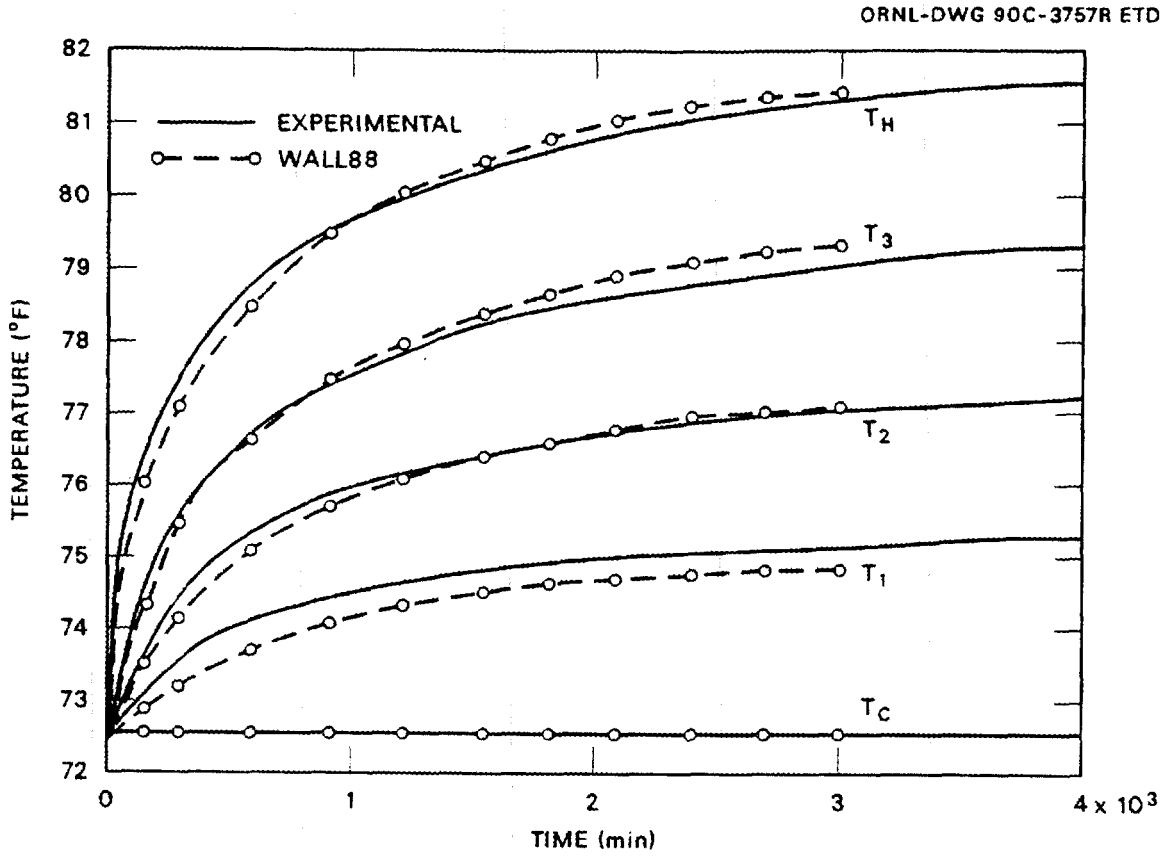

Fig. 12. Comparison of modified WALL88 to experimental transient data.

Potential candidates for heat storage are the binary polyalcohols of AMPL-NPG, NPG-TMP, NPG-PE and NPG-glycerine. Transition temperatures for these combinations range from room temperature to 188°C (370°F) with the flexibility to vary the transition temperature by changing the composition of the particular binary. For example, experiments performed on NPG-10 mol % glycerine binary showed near isothermal behavior at 25°C (77°F), and NPG-10 mol % TMP at 10°C (50°F). Thermal cycling experiments showed in general that the NPG-based binaries were stable; however, plasterboard impregnated with a NPG-based binary showed consistent performance only up to about 170 thermal cycles and by 1500 cycles has lost its latent storage capacity as the PCM had sublimed from the board.

Prior work has shown that PE and NPG can be used as solid-solid TES materials.[8] However, the phase diagram and transition mechanisms were not known and have been revealed through this project. The PE-NPG phase diagram was developed by X-ray

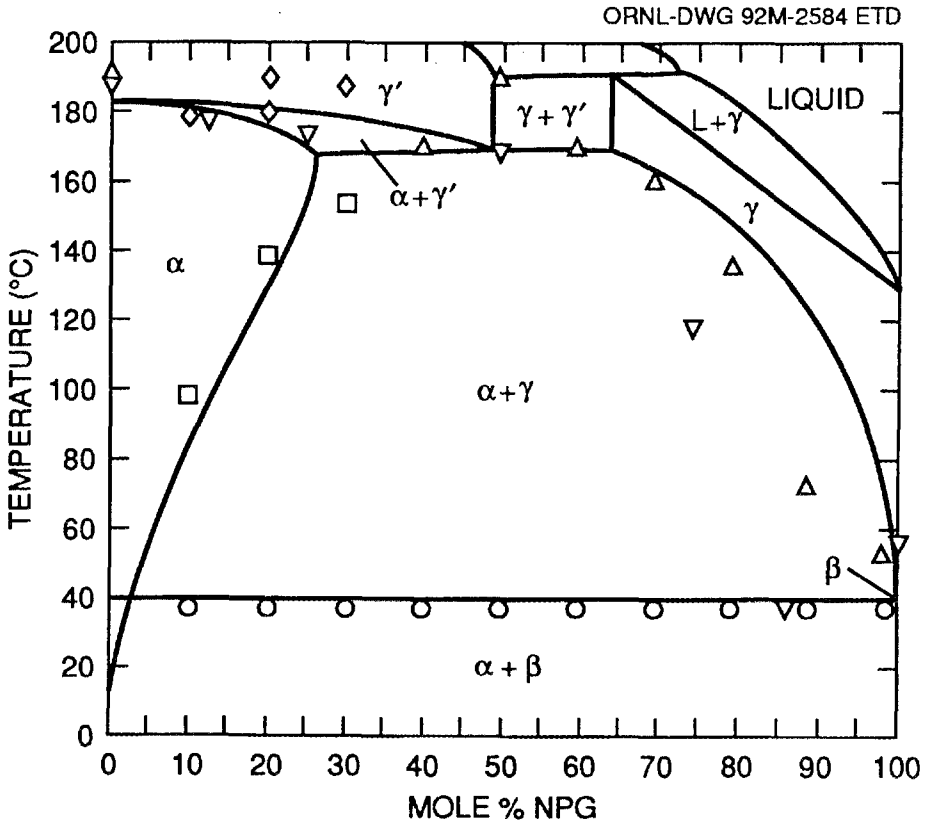

Fig. 13. Phase diagram for PE/NPG system.

diffraction methods and confirmed using the on-line computer program "FACT" offered through McGill University. This program sets up mathematical expressions for the thermodynamic properties of all known phases, and a self-consistent wet of optimized thermodynamic parameters describing the free energies of the compounds (both liquid and solid solutions) is obtained. The phase diagram for the PE-NPG system is shown in Fig. 13. Except for the inverted triangles, the data points shown in Fig. 13 were determined by the University of Nevada-Reno through this study. Data shown as inverted triangles were taken from Benson et al.[8] In NPG-PE binaries rich in NPG, the β phase transforms to γ at a constant temperature, but the transition of PE-rich α to γ' varies as a function of composition. The DSC traces of the NPG-rich binaries showed two normal endotherms $\alpha \rightarrow \gamma'$ and $\beta \rightarrow \gamma'$ and another continuous broad endotherm for the $\alpha \rightarrow \gamma$ transition in the two phase region during heating. It was proposed that these $\gamma \rightarrow \alpha$ transitions are due to changes in the compositions and amounts of phases in this binary. In the binaries rich in PE, $\alpha \rightarrow \gamma$

and $\beta \rightarrow \gamma$ transitions occur as expected, but the energy stored in the β phase at low temperatures is continuously released at a higher temperature due to the $\gamma \rightarrow \alpha$ transformation. Thus, heating of PE-rich binaries results in a heat pump action in which the energy is released at the higher temperature.

A phase diagram was also developed for the AMPL-NPG system to determine the low temperature transitions that could be available for TES applications. The phase diagram

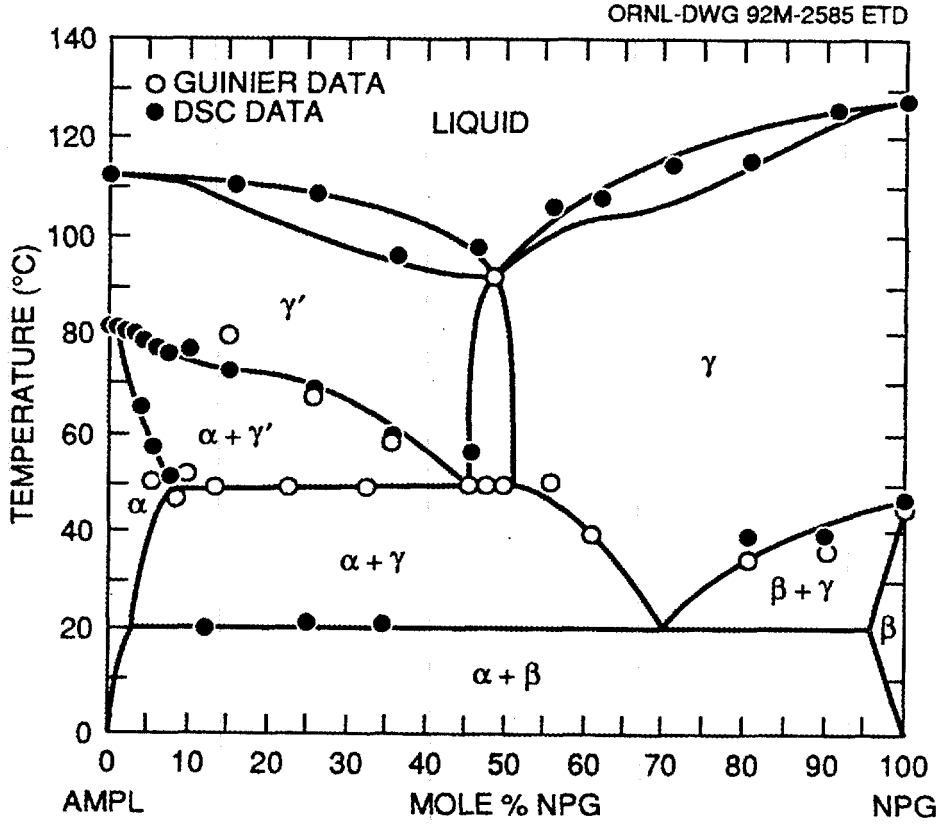

Fig. 14. Phase diagram for the AMPL/NPG system.

developed is shown in Fig. 14. The α and γ' are low and high temperature AMPL-rich phases, and β and γ are low and high temperature NPG-rich phases respectively. The key features of this eutectoidal type phase diagram include the $\alpha + \beta \rightarrow \gamma$ transition at 20° C, $\alpha + \gamma \rightarrow \gamma'$ at 50° C and finally the eutectic $\gamma + \gamma' \rightarrow$ Liquid at about 92° C. It was discovered that two high temperature phases (γ and γ') co-exist in equilibrium in a narrow composition range. It was also found that the AMPL-rich binaries could be supercooled; the high

temperature phase can be triggered by straining or stirring the material to release an estimated 50 to 52 cal/g of heat at room temperature.

The transition temperature of PG was reduced with the addition of TMP and AMPL. these binaries showed two regions with at least two solid-solid transitions. For the PG-TMP system, an 84°C solid-solid transition was recorded for the binaries up to 40 mol % TMP. In the case of the PG-AMPL binary, there were continuous decreases in the transition temperature with increasing additions of AMPL.

3. TECHNICAL PROGRAM - INDUSTRIAL TES

3.1 DEVELOPMENT/TESTING OF TES MEDIA FOR INDUSTRIAL APPLICATIONS

Over a period of several years, the TES program has continued the development of an advanced high temperature TES material for industrial applications. The initial purpose of the material is to capture heat from flue gases in periodic industrial processes, store the energy as sensible and latent heat in a packed bed of the material, and release the heat at a later time back into the industrial process as needed. Therefore, the material provides a compact medium for regeneration of heat by industry. The unique storage material is a ceramic containing a PCM in its microstructure. As the material is carried above the melting point of the PCM, latent heat is stored as the PCM melts in addition to the sensible heat stored in the ceramic matrix and PCM. The large surface area of the ceramic microstructure effectively retains the liquified PCM so that a "form-stable" material with a high effective heat capacity around the PCM melting point is produced. In prior years, the material, a composite PCM or CPCM, was carried through laboratory development. However, the performance of this material when used in a large packed bed storage system with flue gas and air as working fluids was not determined. Further, the thermodynamic performance of a packed bed containing this material had not been verified. A project is currently underway at MSU to design, construct, install and operate a packed bed TES system to study the metallurgical performance of the CPCM and to verify and validate a thermodynamic model of the packed bed system. The purpose of the model is to facilitate optimal designs of a full-scale packed bed systems.

During the reporting period, efforts were continued by MSU toward the near-term objective of building and operating a high temperature packed bed facility for testing the CPCM. Design of the facility, shown schematically in Fig. 15 was completed. The high

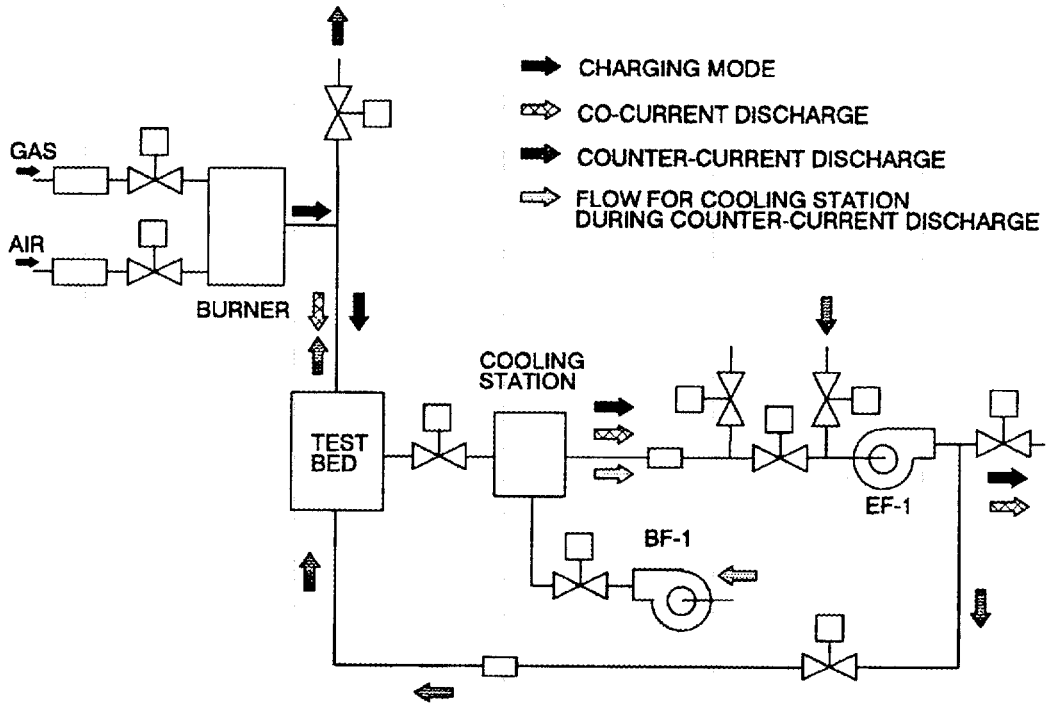

Fig. 15. Schematic of packed bed test facility.

temperature ducting arrangement allows the facility to be operated in both parallel and counterflow modes during discharge. Tests with two diameter pellets [25.4 mm (1 in. maximum dia.)] were needed for a Reynolds number range of 25 - 100 with a gas mass flow rate of 590 kg/h (1300 lb/h). This Reynolds number range covers the likely operating conditions of a prototype system and provides a sufficient span for validation data needed to test the packed bed thermal model developed by MSU.

The test facility design was based on a charging protocol that terminates charging when sufficient energy is accumulated in the test bed to completely melt all the CPCM pellets at their melting point of approximately 710°C (1300°F). Simulations from the packed bed model showed over half of the pellets would be completely melted when charging is

terminated in the manner described. A tentative location for the test facility on the MSU campus was selected, and construction of the facility by McConnell Industries (Birmingham) was begun.

4. CONCLUSIONS

During the reporting period, the diurnal and industrial TES program has made significant progress in the development and application of TES. Coordinated research was performed aimed at four large applications: (1) the development of a low temperature chill TES system for refrigeration applications, (2) the development of an advanced ice storage system for commercial building cooling, (3) development of building materials with enhanced heat capacity, and (4) development of a compact and effective high temperature regenerator technology. In each case, the research performed supports ultimate commercialization of a TES technology. Research to develop the chill TES system was extended to a potential manufacturer who built a 4 ton-h system for testing. It was found that the facilities and equipment needed for fabrication of chill TES systems is a good fit with existing facilities and capabilities. This was an important finding supporting transfer of the chill TES technology from the laboratories at Rocky Research toward a manufacturing base will be straightforward since little outlay will be needed by the manufacturer for additional equipment. It was demonstrated that further work is needed to reduce the solid/vapor heat exchanger cost and performance. As a result of this finding, further work remains underway to optimize this component of the chill TES system.

The prototype direct contact ice storage system developed and tested by CBI proved that the system works reliably and with relatively high evaporator temperatures. Despite this finding, the performance (efficiency) of the direct contact system was poorer than expected. The major loss in efficiency was caused by the compressor used. This liquid ring compressor was originally designed to be used as an air compressor that was simple in design, with few moving parts and capable of accommodating water carryover as is present in the direct contact ice system. It may be possible to employ other compressor designs (e.g. centrifugal or screw) to improve the efficiency of the system provided the carryover and lubrication issues could be resolved. Perhaps more significant is the fact that the direct contact system is based on R-114 as the refrigerant, and as this refrigerant is being phased out, a replacement that (1)

has a saturation pressure/temperature behavior similar to R-114, (2) does not hydrolyze with water appreciably and does not form a clathrate, and (3) is nonflammable and (4) is affordable has not been identified. Further work with the direct contact ice system was postponed until the outlook for improving the system efficiency and identifying a suitable replacement refrigerant is more promising.

There was significant progress made during the reporting period in the development of a PCM wallboard. Fire safety tests conducted by a potential manufacturer showed that in medium concentrations (16 wt. %), the PCM wallboard has the flame spread characteristics of wood. Work to reduce the flame spread and fire safety of the PCM wallboard through the use of nonflammable coatings and fire retardant chemicals either on the surface or in the core of the plasterboard showed that these materials provide only a small improvement and, in most cases studied, smoke generation was worsened. Efforts to develop a method for incorporating the PCM into plasterboard during manufacture were successful in identifying a silica/PCM system that produces a dry powder which can be added as proposed. Work to make the rheology of this additive system similar to that in conventional plasterboard manufacture is continuing. Finally, PCM model validation studies were conducted in which the measured transient thermal response of PCM wallboard to a step change in flux on one face was compared with model predictions. In the case of a step increase in the temperature of one face, good agreement between model and experiment was obtained when the thermophysical property data for the PCM wallboard was taken from a DSC scan. This scan showed that the paraffin used in the plasterboard melts over a small temperature range rather than at a single temperature as suggested by theory. This work suggests that results from a DSC give the best representation of the thermophysical property values applicable to a model of the melting process rather than "textbook" values.

Finally, research to study the performance of the high temperature CPCM for a packed bed regenerator took a major step forward with completion of the design of a facility for testing this material under actual flue gas conditions. A thermodynamic model was used to determine critical test parameters and to select the configuration for the packed bed. Fabrication of this test facility has commenced.

REFERENCES

1. U. Rockenfeller and L. Kirol, *Development of a Complex Compound Chill Storage System*, ORNL/Sub/86-57432/1, August 1991.

2. J. J. Tomlinson, *Thermal Energy Storage Technical Progress Report April 1989-March 1990*, ORNL/TM-11819, March 1991.

3. R. Petri, E. Ong, A. Kardas, *Development of Composite Latent/Sensible Heat Storage Media*, ORNL/Sub/86-95001/1, December 1990.

4. T. K. Stovall, *Turbo Refrigerating Company Ice Storage Test Report*, ORNL/TM-11657, June 1991, Oak Ridge National, Laboratory.

5. R. J. Kedl, *Wallboard with Latent Heat Storage for Passive Solar Applications*, ORNL/TM-11541, May 1991.

6. A. Solomon, V. Alexiades, and D. G. Wilson, *The Mathematical Modeling of Melting and Freezing Processes*, Hemisphere Press (1990).

7. H. S. Carslaw and J. C. Jaeger, *Conduction of Heat in Solids*, Oxford University Press, London, England, 2d ed., 1959.

8. D. K. Benson, R. W. Burrows and J. D. Webb, *Solar Energy Materials*, 13, 1986, 133-152.

ORNL/TM-12081
Dist. Category UC-202

Internal Distribution

1. T. D. Anderson
2. R. S. Carlsmith
3. J. E. Christian
4. W. G. Craddick
5. J. B. Drake
6. W. Fulkerson
7. J. A. Getsi
8. J. E. Jones Jr.
9. L. Jung
10. M. A. Kuliasha
11. W. R. Mixon
12. M. Olszewski
13. A. E. Ruggles
14. A. C. Schaffhauser
15. M. Siman-Tov
16. T. K. Stovall
17. M. J. Taylor
18-22. J. J. Tomlinson
23. A. Zucker
24. ORNL Patent Office
25. Central Reference Section
26. Document Reference Section
27-28. Laboratory Records Department
29. Laboratory Records (RC)

External Distribution

30. Kevin Drost, Battelle Pacific Northwest Laboratories, P. O. Box 999, Battelle Boulevard, Richland, WA 99352
31. Russ Eaton, Advanced Utility Concepts Division, U. S. Department of Energy, CE-142, Forrestal Building, 1000 Independence Avenue, Washington, D. C. 20585
32. D. E. Gound, Program Manager, Research management Branch, U.S. Department of Energy, ORO, Box 2001, Oak Ridge, TN 37831-8611
33. Landis Kannberg, Battelle Pacific Northwest Laboratories, P. O. Box 999, Battelle Boulevard, Richland, WA 99352
34. Kurt W. Klunder, Director, Office of Energy Management, Office of Utility Technology, U.S. Department of Energy, CE-14, Forrestal Building, 1000 Independence Avenue, Washington, D. C. 20585
35. Don Neeper, Advanced Engineering Technology Group, Los Alamos National Laboratory, MS J567, Los Alamos, NM 87545
36. Eberhart Reimers, Advanced Utility Concepts Division, U.S. Department of Energy, CE-142, Forrestal Building, 1000 Independence Avenue, Washington, D. C. 20585
37. Robert L. San Martin, Office of Utility Technology, U.S. Department of Energy, CE-10, Forrestal Building, 1000 Independence Avenue, Washington, D. C. 20585
38. Paul Shipp, U.S. Gypsum Corporation, Research Center, 700 N. Highway 45, Libertyville, IL 60048
39. Chang W. Sohn, Energy Systems Division, U.S. Army Construction Engineering Laboratory, Corps of Engineers, Box 4005, Champaign, IL 61824-4005
40. R. D. Wendland, Project Manager, Thermal Storage Technology, Electric Power Research Institute, 3412 Hillview Avenue, P.O. Box 10412, Palo Alto, CA 94303
41. Office of Assistant Manager for Energy Research and Development, Department of Energy, ORO, Oak Ridge, TN 37831

42-53. Given distribution as shown in DOE/TIC-4500 under Category UC-202 (Thermal Energy Storage)